BEHAVIOUR OF THE SUBWAY TUNNEL IN ALGIERS: PHYSICAL MODEL EXPERIMENTAL STUDY

ABDELBAKI SERIANI, Y. KISMOUNE THÉSARD and TAYEB SERRADJ

About the authors

Abdelbaki Seriani
Genius University Badji Mokhtar,
Faculty of Science of the Ground
BP 12, 23000 Annaba, Algeria
E-mail: seriani7@yahoo.fr

Y. Kismoune Thésard
Genius University Badji Mokhtar,
Faculty of Science of the Ground
BP 12, 23000 Annaba, Algeria

Tayeb Serradj
Genius University Badji Mokhtar,
Faculty of Science of the Ground
BP 12, 23000 Annaba, Algier

Abstract

Tunnel construction projects are too expensive to be approached directly without a preliminary small-scale model study and subsequent verification with a mathematical model, if needed. These studies enable to avoid unforeseen consequences which emerge at the time of the project realization. It is within this framework that we carried out our investigations. The behaviour of a subway tunnel in Algiers and the state of transition of the surrounding ground during digging are studied from an experimental point of view via a 1/20 physical model scale.

Keywords

tunnel, equivalent material, physical modelling, supports, deformations, rupture, loosened zone

1 GOALS OF THE INVESTIGATIONS

The lack of experimental data on the tunnel in Algiers (Batch 5) deprive us of a comparison base between measurements and observations carried out in situ and the results obtained by the physical model used within the framework of this research. Nevertheless, the work that we present will be highly useful, being the first approximation of the prospects of the subway tunnel in Algiers. The below methods and the reasons were considered in the investigation:

- the use of artificial rock medium corresponding perfectly to in situ conditions;
- the technology of tunnel construction proposed by the project which will be completely respected during the realization of the tunnel model;
- the digging will be carried out under the load which corresponds to actual weight of artificial material.

This method of investigation (technology and construction of the tunnel model under constant load) provides a better simulation model, much closer to the in situ conditions.

2 THE TASK TO BE SOLVED

This work is aimed at reporting about the aptitude of physical modelling in tunnel projects considering tender ground conditions. To achieve this, the following is considered:

- Measurement of convergence after each stage of construction.
- Observation of the ground movement around the tunnel after each phase, owing to the numerous reference marks placed in artificial material. These marks allow us to measure relative displacements and thus to calculate deformations and specify the state of material around the tunnel model.

– Qualitative verification of combining the supporting systems used.
– Conception of a physical model to carry out the observations and measurements. A mixture of industrial powder is used as artificial rock material.

3 PHYSICAL MODELLING

3.1 CHOICE OF THE PHYSICAL MODEL

To simulate the subway tunnel in Algiers (Batch 5), a physical model was used (Fig. 1), which has two essential advantages:

– Economic advantage from the point of view of construction, and
– Simplicity from the point of view of uses and operation.

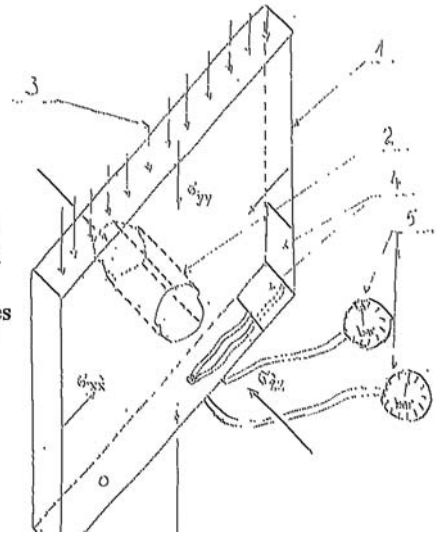

Figure 1. Physical model.

3.2 CHOICE OF THE SCALES OF SIMULATION

We think that it is preferable to choose geometrical scales and scales of equal constraints to avoid complicating the choice of the material equivalent or to have additional loads applied in order to compensate for high values of the voluminal mass in the case of a high scale constraint compared to the 1 : 20 geometrical scale selected. With this scale the width of the tunnel model (50 cm) does not exceed 1/3 of the width of the model (180 cm), as recommended from experience (in order to avoid the influence of borders on the test results).

The calculation of the scales is shown in Table 1 (see next page).

Physical simulation won large applications since an international symposium in Italy on the physical modelling in geomechanics. Certain researchers approached the physical simulation in tunnelling by using different equivalent materials for the rocks and the systems of supports. Thus, for modelling the behaviour of a tunnel, equivalent materials such as:solids (bentonite, mica baryte, ground cork) and binders (paraffin oil, silicon oil) are used (Sauer, 1979). In order to simulate a tunnel in tender rock a mortar of water, cement , bentonite, and sand is used. Another mixture composed by cement, lime quick, sand, and water (Gajàry, 1990) was used for studying experimentally the stability of a roadway.

The simulation of the tunnel supports in appropriate conditions with different equivalent materials is summarized below.

Authors	Type of supports	Equivalent material
Tazawa.Y	Rock bolts	Cooper screws of variable length located at convenient relative distances
	Lining	Mortar of cement with a resistance to compression σc = 20-30 MPa
Adachi .T. & al.	Rock bolts and lining	Kint paper of variable thickness and resistance

In the light of these and other studies (Stimpson, 1968), and based on the criteria listed below (Baron and Larocque; 1960):

- the facility of fabrication of the proposed model,
- relative expenses for the material and the equipment, and
- environmental and security criteria will be observed too.

The author introduces new equivalent materials, such as industrial talk mixed with water.

Industrial talk mixed with water possesses plastic properties similar to in situ conditions (clay-marly soil). The mixture in question is simple (talk + % water), which renders this material recoverable, hence reusable, and therefore cheap.

Physical and mechanical properties of equivalent materials of the rock and of supporting are presented in table 2 on page 28 (Seriani, 1993).

Table 1. Scales of constraints compared to the geometrical scales.

Geometrical scale			Scale of stresses										
Insitu		Model	Insitu			Models								
Dimensions			Dimensions										
Names	Values	Value according to the scale	Names	Symbol	Units	1/40	1/30	1/25	1/20	1/15	1/4	1/3	1/2	1/1.5
L/m Length	1	L	Stress	σ	N/m^2									
			Force	F	NR									
H/m Depth	20	H	Unit weight	γ	Kg/dm^3									
			Accel. gravity	G	$Kg.m/s^2$	Model N°1	Model N°2	Model N°3	Model N°4	Model N°5	Model N°6	Model N°7	Model N°8	Model N°9
W/m Width	10	W	Young modulus	E	N/m^2									
			Poisson coef.	ν	-									
b/m Height	11	b	Friction angle	φ	degree									
			Cohesion	C	N/m^2									
		1/40		σ		1/40	1/30	1/25	1/20	1/15	1/4	1/3	1/2	1/1.5
				F		1:6400	1:480	1:40000	1:32000	1:24000	1:6400	1:4800	1:3200	1:2400
		0.5		γ		1:1	1,33:1	2:1	2:1	2,66:1	10:1	13,3:1	20:1	26,6:1
				G		1:1	1:1	1:1	1:1	1:1	1:1	1:1	1:1	1:1
		0.25		E		1:40	1:30	1:25	1:20	1:15	1:4	1:33	1:2	1:1,5
				ν		1:1	1:1	1:1	1:1	1:1	1:1	1:1	1:1	1:1
		0.25		φ		1:1	1:1	1:1	1:1	1:1	1:1	1:1	1:1	1:1
				C		1:40	1:30	1:25	1:20	1:15	1:4	1:3	1:2	1:1,5
		1/30				1:36000	1:27000	1:25500	1:18000	1:1350	1:3600	1:2700	1:1800	1:1350
						1:1,33	1:1	1,2:1	1,5:1	2:1	7,5:1	10:1	15:1	20:1
		0.66				1:1	1:1	1:1	1:1	1:1	1:1	1:1	1:1	1:1
						1:40	1:30	1:25	1:20	1:15	1:4	1:3	1:2	1:1,5
		0.33				1:1	1:1	1:1	1:1	1:1	1:1	1:1	1:1	1:1
						1:1	1:1	1:1	1:1	1:1	1:1	1:1	1:1	1:1
		0.35				1:40	1:20	1:25	1:20	1:15	1:4	1:3	1:2	1:1,5
		1/25				1:2500	1:18750	1:15625	1:12500	1:9735	1:2500	1:1875	1:1250	1:937,5
						0,625:1	0,833:1	1:1	1,253:1	1,66:1	6,25:1	8,3:1	12,5:1	16,6:1
		0.8				1:1	1:1	1:1	1:1	1:1	1:1	1:1	1:1	1:1
						1:1	1:1	1:1	1:1	1:1	1:1	1:1	1:1	1:1
		0.4				1:40	1:30	1:25	1:20	1:15	1:4	1:3	1:2	1:1,5
						1:1	1:1	1:1	1:1	1:1	1:1	1:1	1:1	1:1
		0.44				1:1	1:1	1:1	1:1	1:1	1:1	1:1	1:1	1:1
						1:40	1:30	1:25	1:20	1:15	1:4	1:3	1:2	1:1,5
		1/20				1:16000	1:12000	1:1000	1:8000	1:6000	1:1600	1:1200	1:800	1:600
						1:2	1:1,5	0,8:1	1:1	1,33:1	15:1	6,66:1	10:1	13,3:1
		1				1:1	1:1	1:1	1:1	1:1	1:1	1:1	1:1	1:1
						1:40	1:30	1:25	1:20	1:15	1:4	1:3	1:2	1:1,5
		0.5				1:1	1:1	1:1	1:1	1:1	1:1	1:1	1:1	1:1
						1:1	1:1	1:1	1:1	1:1	1:1	1:1	1:1	1:1
		0.55				1:40	1:30	1:25	1:20	1:15	1:4	1:3	1:2	1:1,5
		1/15				1:9000	1:6750	1:5625	1:4500	1:3375	1:900	1:675	1:450	1:337,5
						1:2,66	1:2	0,6:1	1:1,33	1:1	3,75:1	5:1	7,5:1	10:1
		1.33				1:1	1:1	1:1	1:1	1:1	1:1	1:1	1:1	1:1
						1:40	1:30	1:25	1:20	1:15	1:4	1:3	1:2	1:1,15
		0.66				1:1	1:1	1:1	1:1	1:1	1:1	1:1	1:1	1:1
						1:1	1:1	1:1	1:1	1:1	1:1	1:1	1:1	1:1
		0.73				1:40	1:30	1:25	1:20	1:15	1:4	1:3	1:2	1:1,5

Table 2. Mechanical properties of the mixture.

Geomechanical parameters	Symbols	Units	In situ values of marly clay	Laboratory tests results	Values required by scale (1/20)
Compressive strength	σ	kPa	270.0-600.0	30.0-50.0	13.5 30.0
Young's modulus	E	kPpa	9000-40000	368.0-520.0	450-2000
Internal friction angle	Φ	degree	18-30	29.6	30
Cohesion	C	kPa	100-110	56.8	50-55
Weight unit mass	γ	kg/m^3	1.6	1.6	1.6
Poisson's coefficient	ν	-	0.45	0.40-0.45	0.45

Table 3. Mechanical properties of a support model (scale 1/20).

Kind of support	Mechanical and geometrical parameters	In situ values	Laboratory test results	Values required by scale
Bolting (soldering wire)	Tensile strength	275 MPa	21.49 MPa	13.75 MPa
	Length	3- 4 m		0.15 – 0.20 m
	Acting air	1.4 m^2		0.0035 m^2
Shotcrete (mixture of gypsum, quick lime, water and inert material [according to A.M.Kozuna 1957])	Compressive strength	21.0 MPa	1.05 MPa	1.05 MPa
Steel arches (very fine aluminium strips transformed in segments with a transversal U section)	Moment	108750 N.m	1.36N.m	1.36 N.m
	Transversal section width	180 mm		9.0 mm
	Distance between two successive steel arches	1.2 m		0.06 m

The materials for the simulation of different types of supports described above are not convenient for the artificial rocks used in our conditions owing to construction technology of the tunnel model (construction under a constant load, in extremely wet conditions, hence in very soft artificial rocks.)

The equivalent materials for simulating tunnel supports used in our case and their mechanical properties are shown in Table 3.

3.3 EXPERIMENTAL METHODOLOGY

The compacted equivalent material is placed in the model with the following dimensions:

- height: 110 cm
- extent: 180 cm, and
- thickness: 20 cm.

Black reference marks are established horizontally in the artificial material, white reference marks are stuck on Plexiglas just above the black reference marks. The black reference marks are mobile and react to artificial rock displacement, while the white reference marks are fixed. These reference marks are photographed after each phase of construction (after it has undergone displacements). After consolidation, the model of tunnel is excavated to the thickness of 7cm representing the distance between the steel arches. The execution time of pickling and installation of the supporting systems is approximately three hours. The nomenclature of different tunnel cutting phases is as follows:

- Phase I: Cutting a working place in the excavation roof to a depth equal to rib spacings.
- Phase II: Installing rock bolts and a superior rib arch
- Phase III: Concrete projection
- Phase IV: Cutting a work place in the lower part of the excavation to a depth equal to rib spacings.
- Phase V: Installing the inferior rib arch
- Phase VI: Concrete projection on the lower part of the excavation.

In the model, the various phases of the superior section are represented successively in Figs. 2-7.

Figure 2. Cutting the first slice of the superior section.

Figure 3. Appearance of deformation.

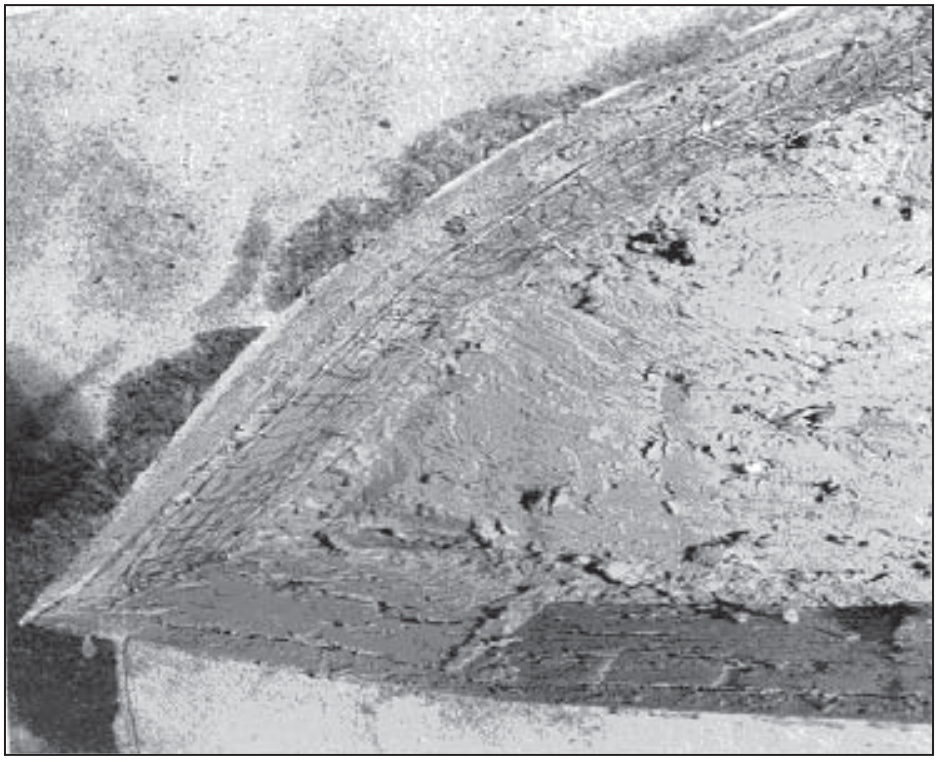

Figure 4. Installation of bolts and steel fabrics.

Figure 5. Installation of steel arches.

Figure 6. Projection of shotcrete.

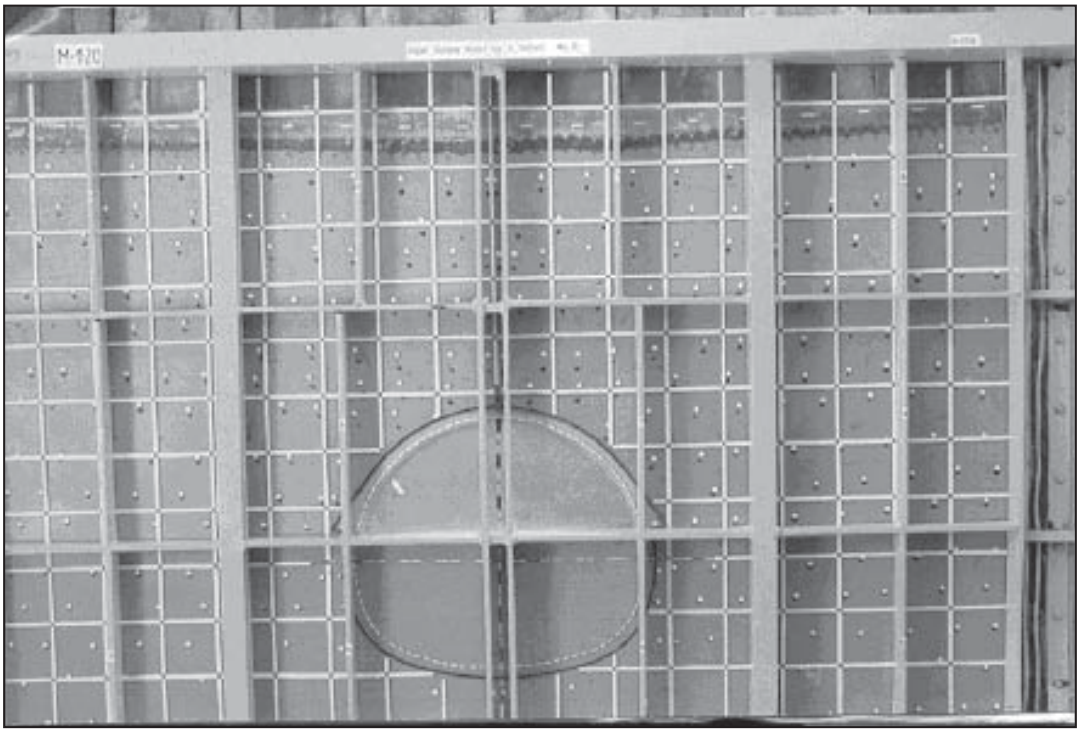

Figure 7. Completion of the higher section.

Deformations after each construction phase of the first section are illustrated in Fig. 8.

All these construction operations are repeated during the digging of other sections. However, it should be noted that a crack appeared in the shotcrete of the first section after the completion of the second section digging. This crack was prolonged after concreting the third section which presupposed the formation of a disturbed zone on the roof of the tunnel model (Fig. 9).

Various construction stages in successive diggings of the lower section are presented in Figs. 10–13.

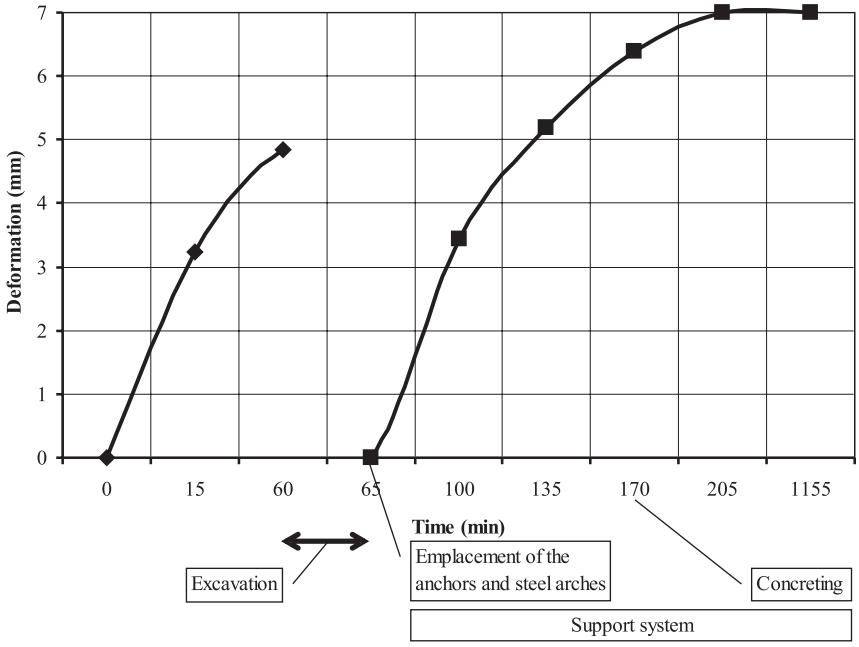

Figure 8. Evolution of the deformation at the end of the first section.

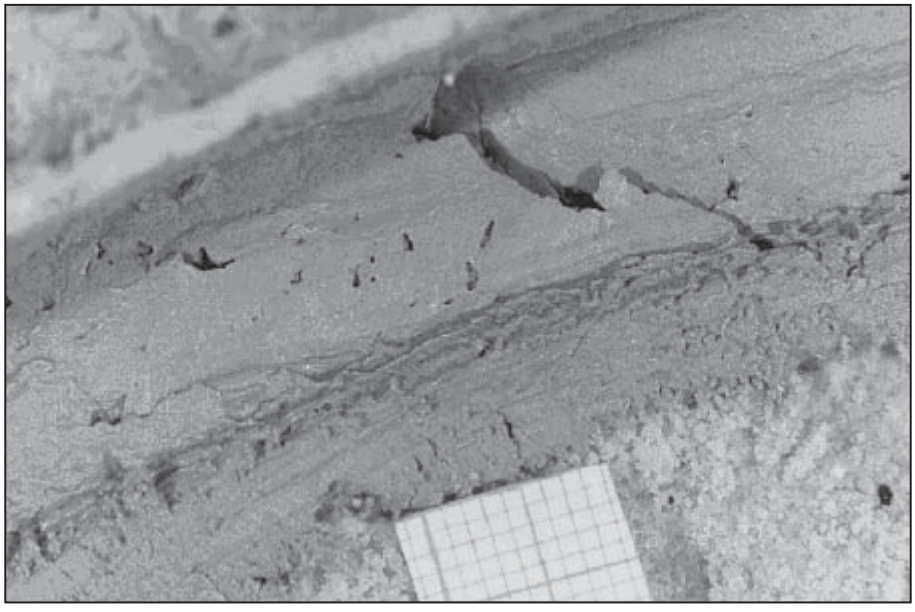

Figure 9. Appearance of a disturbed zone on the roof of the model.

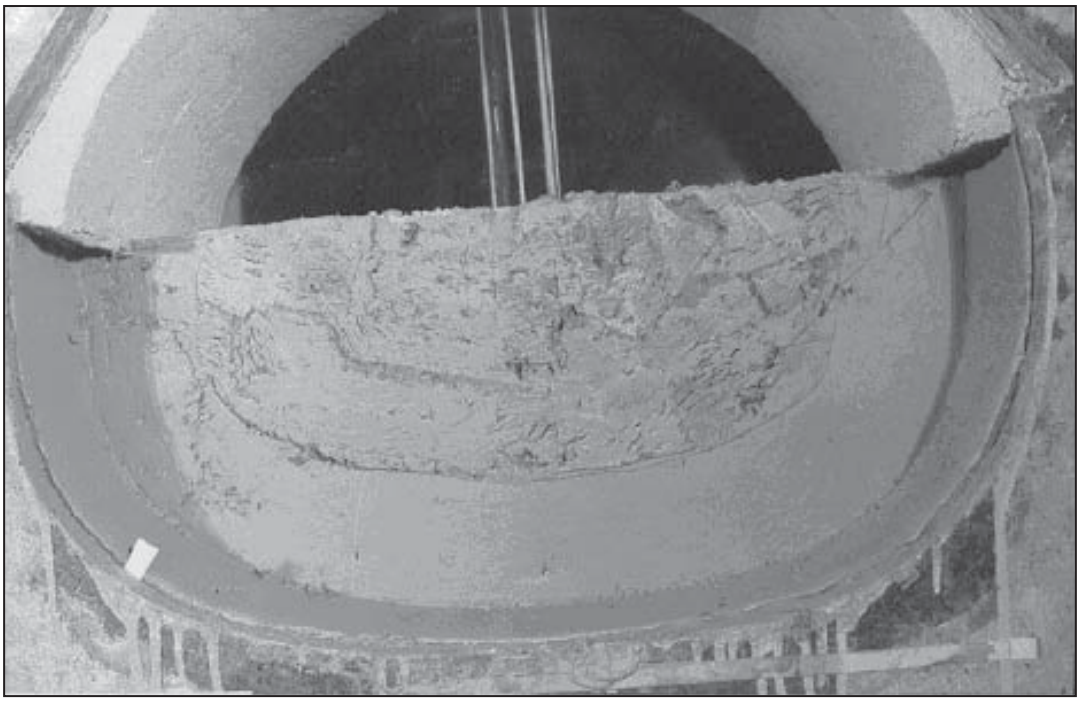

Figure 10. Cutting of the first slice of the inferior section.

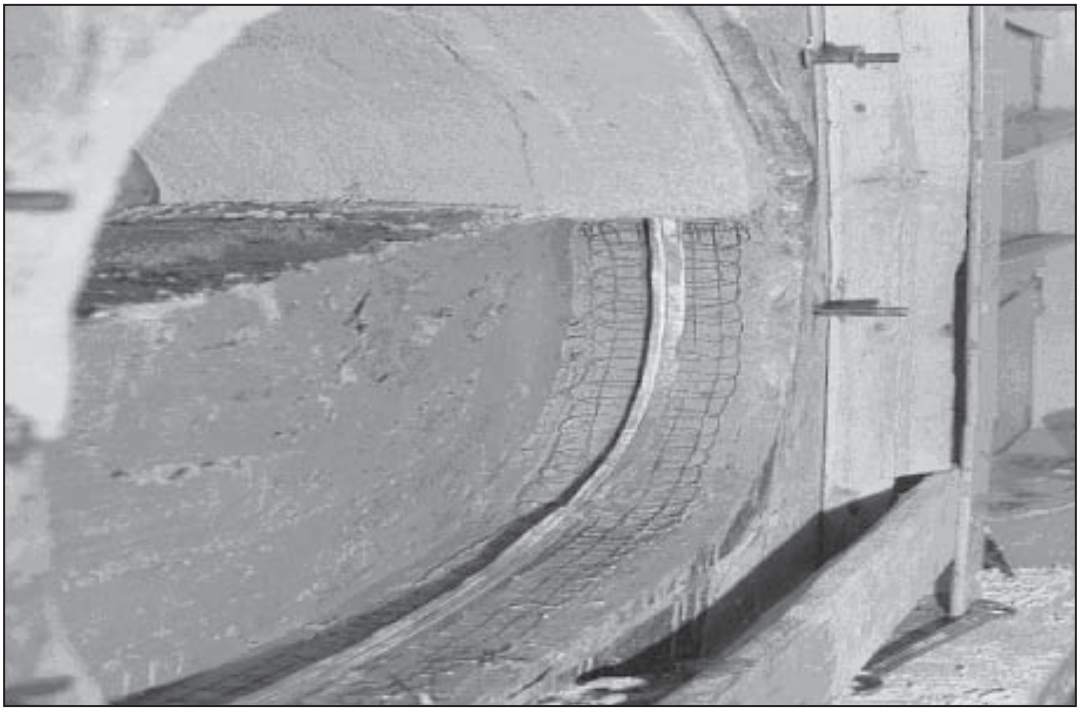

Figure 11. Installation of steel fabrics and steel arches.

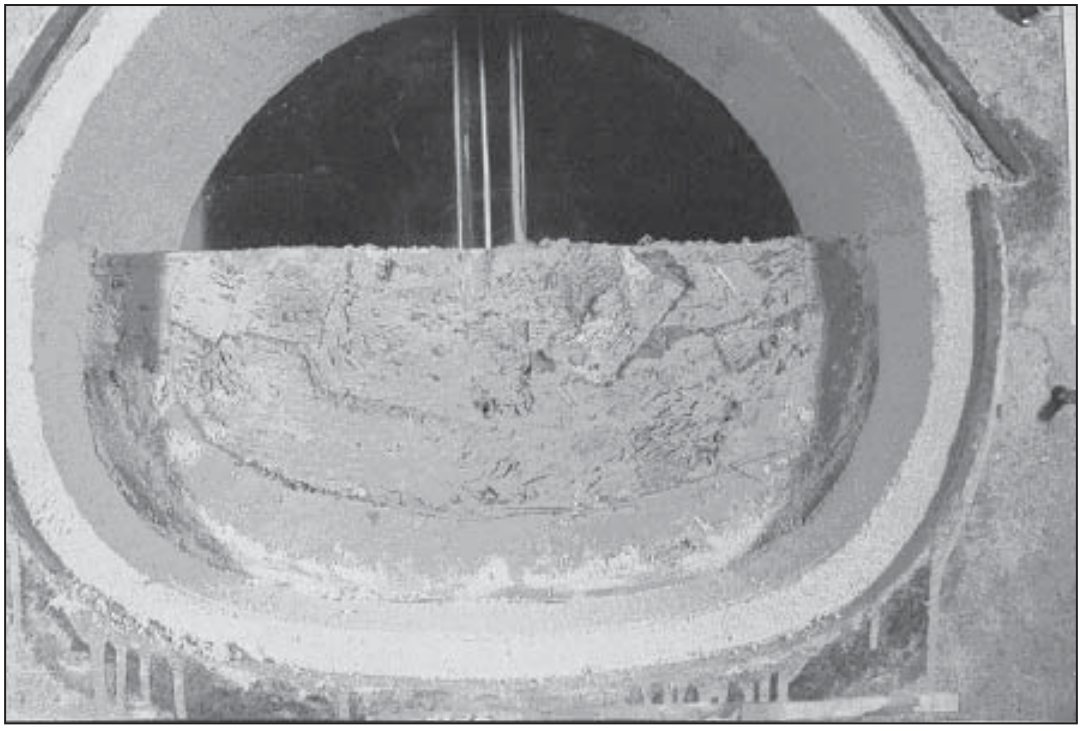

Figure 12. Concreting the first slice of the inferior section.

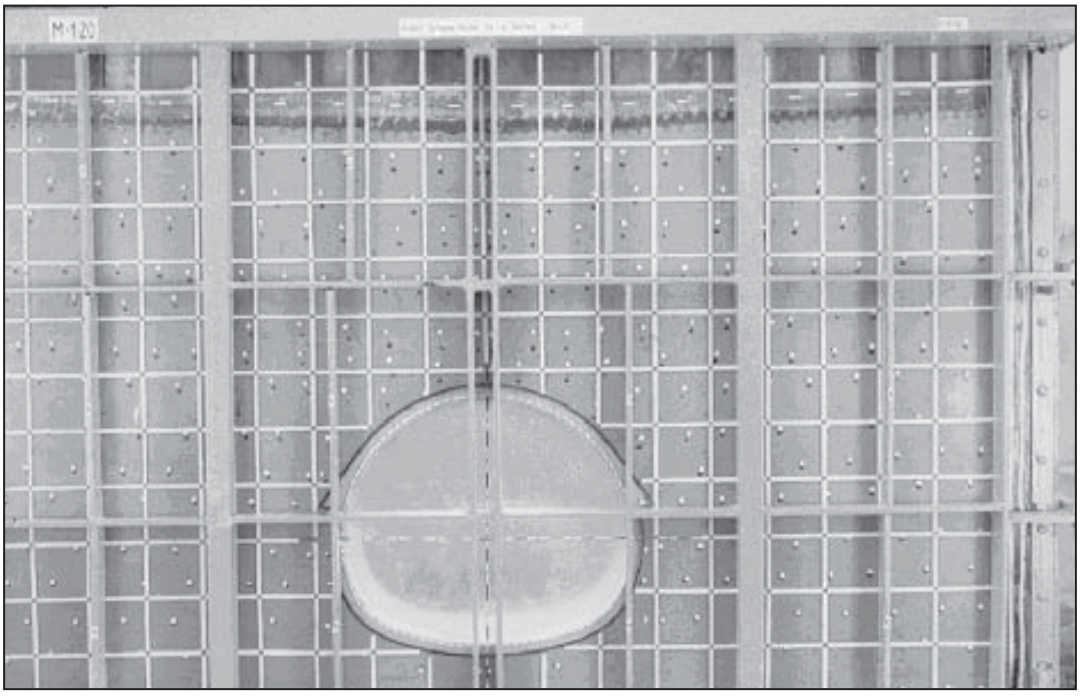

Figure 13. Final construction of the model.

Time evolution of the deformations is shown in Fig. 14.

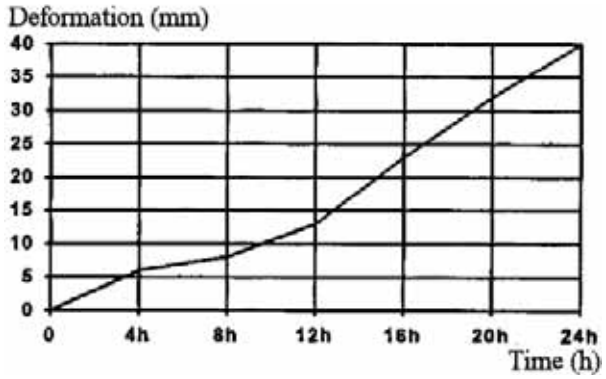

Figure 14. Convergence of the model according to time.

The measurement method of displacements is an optical method leading to misreadings of those reference marks especially which are far away from the centre of the model as shown in Fig. 15.

The coefficient of correction is calculated as follows:

A mesh of white squares on the model has a width of 10cm, which is 2cm on the photograph. This dimension corresponds to an opening of 19 units on the optical glass objective. These 19 units measure 1.9mm on the photograph, so the scale between the model and the photo is of 1:5 and the scale between the photo and the optical glass is of 10:1. The measurement scale thus becomes of 10:5, therefore 2:1, from which 14 units correspond to 10.5mm. The correction coefficients are presented in Table 4.

Table 4. Correction coefficients of measured displacements.

Coordinate X	Correction	Coordinate Y	Correction
0	-3.6	0	2.4
10	-3.2	10	2.0
20	-2.8	20	1.6
30	-2.4	30	1.2
40	-2.0	40	0.8
50	-1.6	50	0.4
60	-1.2	60	0.0
70	-0.8	70	-0.4
80	-0.4	80	-0.8
90	0.0	90	-1.2
100	0.4	100	-1.6
110	1.2	110	-2.0
120	1.6	120	-2.4
130	2.0		
140	2.4		
150	2.8		
160	3.2		
170	3.6		

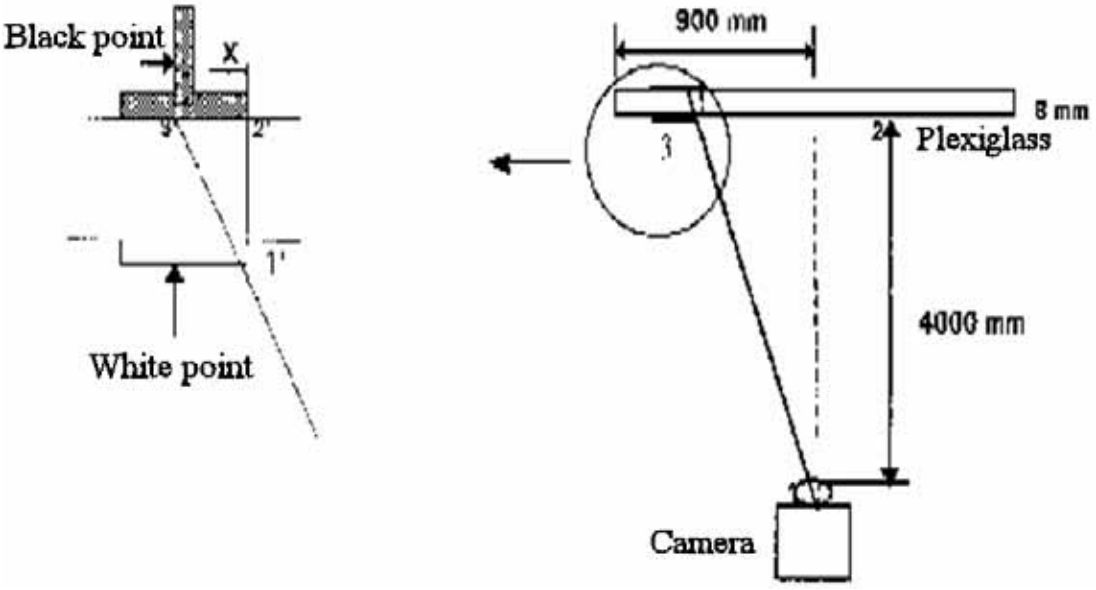

Figure 15. Concreting the first slice of the inferior section.

4 CALCULATION OF THE VOLUMETRIC AND ANGULAR DEFORMATIONS

Many significant problems require constraints and elongations in the x-y plan although the constraints σ_{zz} can exist; σ_{xz} and σ_{yz} have been neglected in our case. If it is supposed that our model is one elastic unit yet sufficiently subjected to constraints which prevent sound movement, no particle displacements are possible inside the model without the model deformation. Small displacements of the model particles are usually presented by the components u and v for a problem of plane deformation. These represent the displacements of the reference marks established in the model. Their measurement method is described later on. Elongations for such a problem are:

$$\varepsilon_{xx} = \frac{\partial u}{\partial x} \qquad (1)$$

$$\varepsilon_{yy} = \frac{\partial v}{\partial y} \qquad (2)$$

$$\theta_v = \varepsilon_{xx} + \varepsilon_{yy} \qquad (3)$$

$$\gamma_{xy} = \frac{\partial u}{\partial y} + \frac{\partial v}{\partial x} \qquad (4)$$

$$\gamma_{xy}^{\max} = \sqrt{\left(\varepsilon_x - \varepsilon_y\right)^2 + \gamma_{xy}^2} \qquad (5)$$

The pictures show the isolines of expansion after digging and supporting each section.

The negative sign indicates the areas of extension while the positive sign indicates the areas of compression. That is how two compression zones of low intensity are formed at the end of the first slice in laterally anchored areas.Their value is of 1% . An extension zone starts to appear on the crown of the tunnel (Fig. 16).

Fig. 16 reflects the state of material when the higher section of the tunnel is completed. It is evident from Fig. 16 that the zones of high compression located in the previously quoted areas have moved to lower un-anchored areas. In turn, the inside of the stross is compressed. The extension area is amplified to reach a value of 3%. Laterally anchored areas have undergone a compression of 6% just above the crown. The area compressed earlier has slackened and has given rise to a disturbed zone. On the level of stross, compression reached 4% (Fig. 17 on next page).

Fig. 18 (on next page) shows a value of a maximum distortion which almost equals the one in the model of an intensity of 6°.

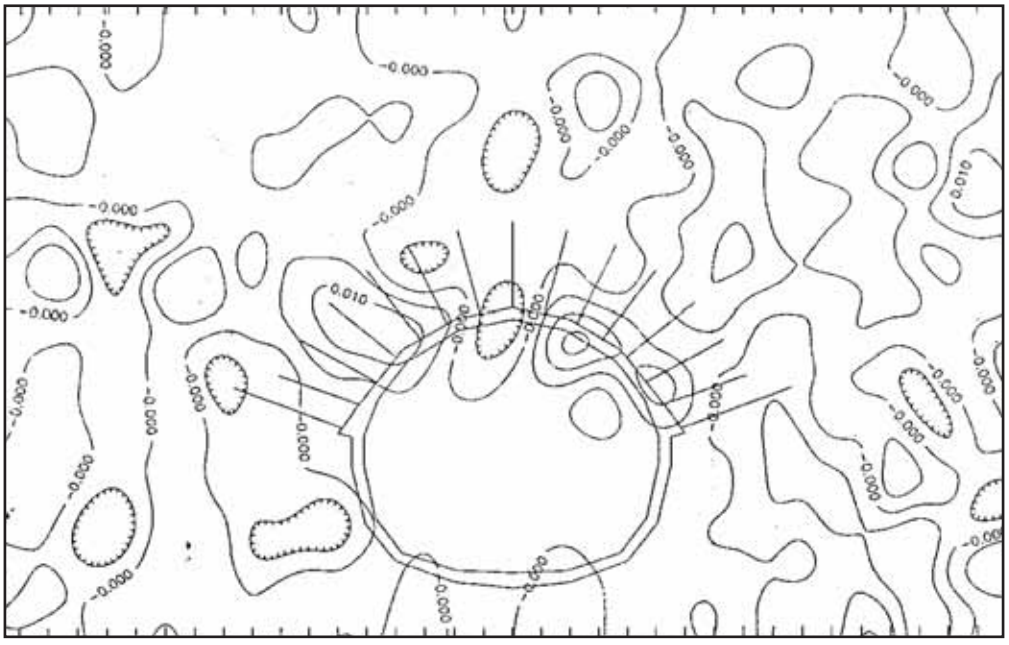

Figure 16. State of elongations at the end of the first slice.

Fig. 19 (on page 38) shows a maximum distortion of 4° at the end of the third slice. The distortion concerning this training course is much larger, it is 4°. On the crown of the tunnel model it is 3°. The rocks with the same distortion are similar to concentric boxing rings around the centre of the higher section floor of the tunnel model.

The excavation and the supporting of the tunnel model are finished with the completion of the sixth slice. Fig. 19 shows the state of the material around the tunnel model; below the stross, on its walls and at the anchoring level, the material is in a compression state. Above the crown, the extension is always of the same intensity, hence a permanent existence of a disturbed zone (Fig. 20, page 38).

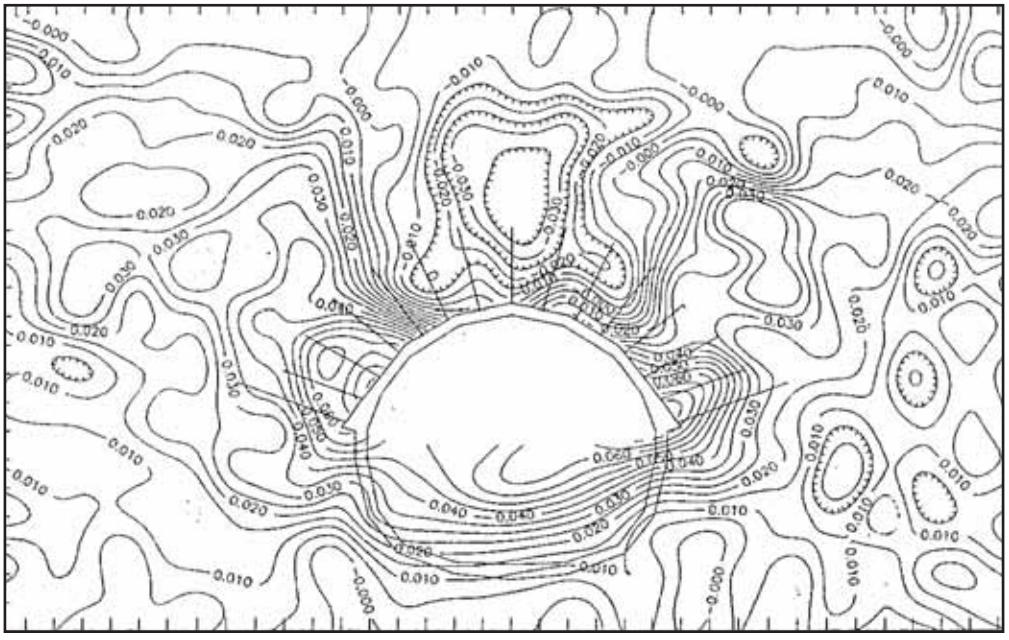

Figure 17. State of elongations at the end of the third slice.

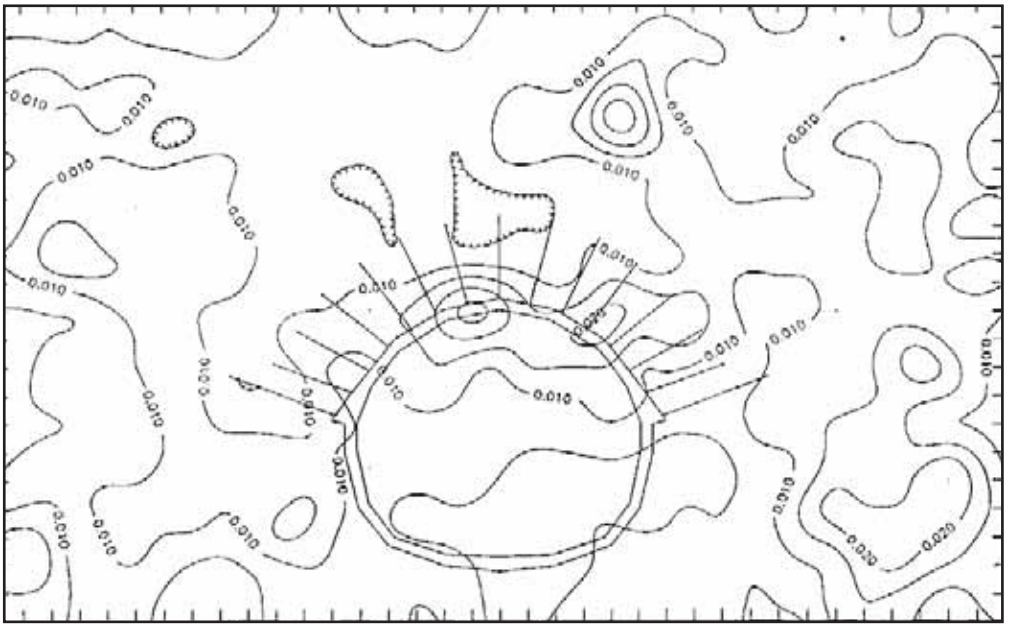

Figure 18. State of distortions at the end of the first slice.

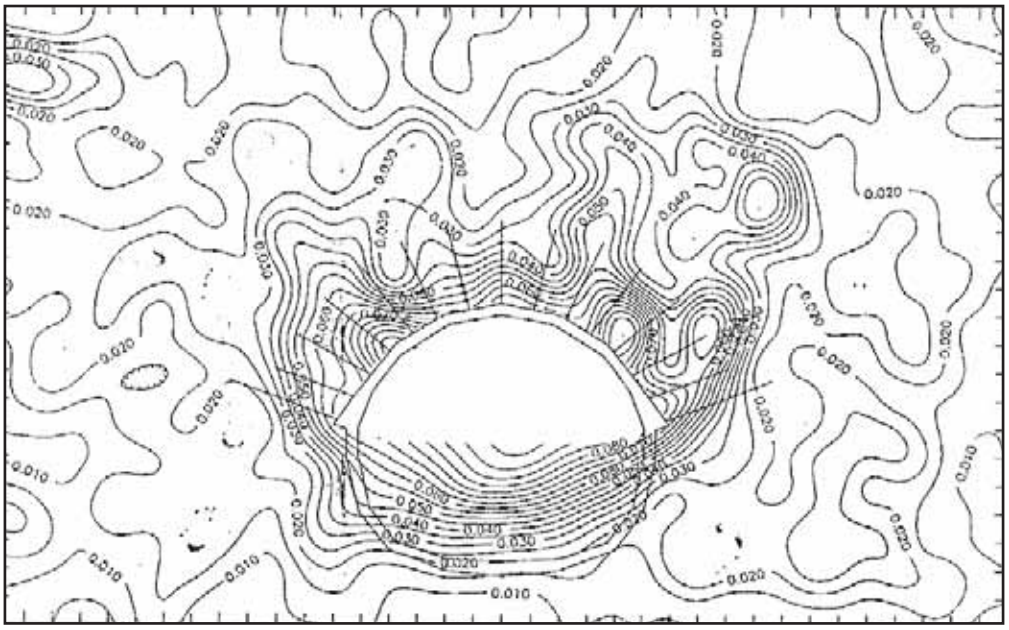

Figure 19. State of distortions at the end of the third slice.

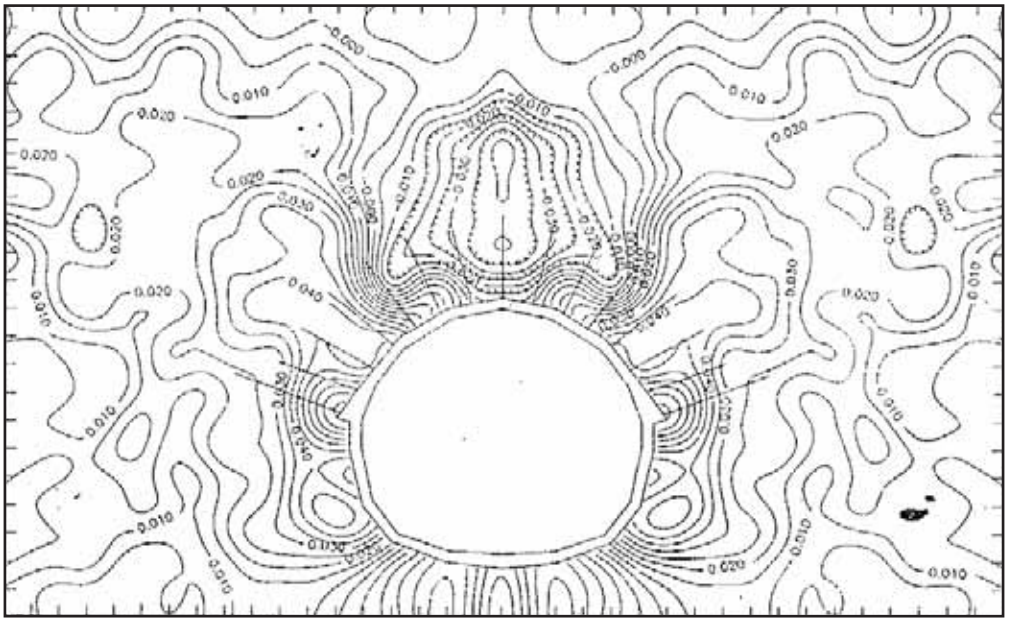

Figure 20. State of elongations at the end of the sixth slice.

Fig. 20 represents the state of distortions when the tunnel model is fully completed. Laterally anchored areas of the higher section remain subjected to a distortion equal to 3.43°, while the value of γ max does not exceed 3° on the crown level and it is even lower around the stross (Fig. 21, next page).

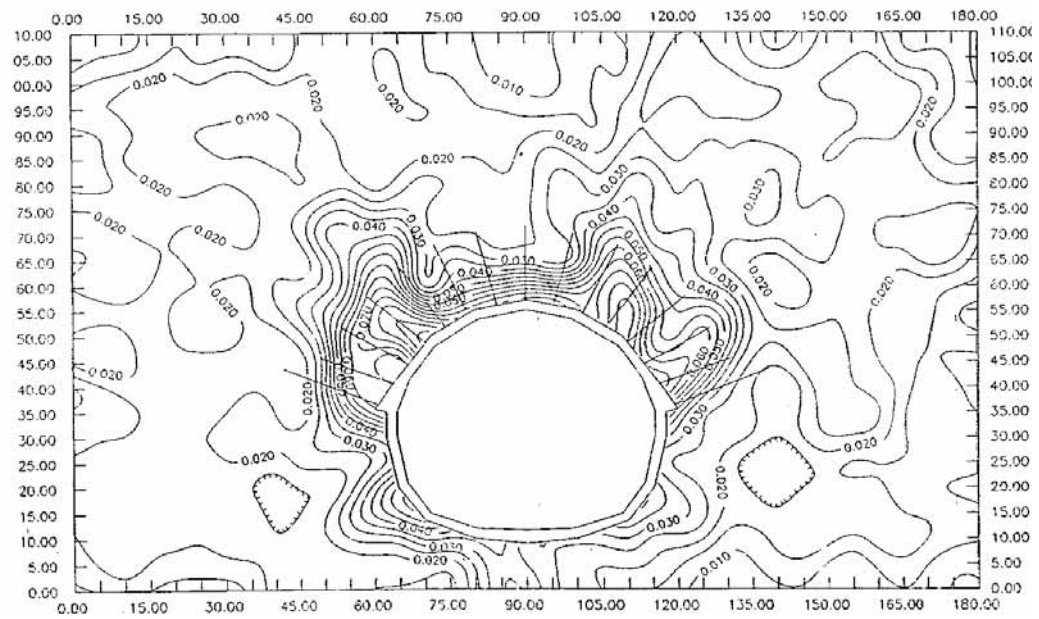

Figure 21. State of distortions at the end of the sixth slice.

5 EVALUATION OF THE PLASTIC ZONE

The fundamental equations are taken from Sakurai S. (1985).

From Hook's law

$$\varepsilon_1 \cdot E = \sigma_1 - \nu \cdot \sigma_3 \qquad \varepsilon_3 \cdot E = \sigma_3 - \nu \cdot \sigma_1 \qquad (6)$$

we obtain the deviatoric of the deformation

$$\varepsilon_1 - \varepsilon_3 = \frac{1+\nu}{E}(\sigma_1 - \sigma_3) \qquad (7)$$

and the volumetric elongation

$$\varepsilon_1 + \varepsilon_3 = \frac{1+\nu}{E}(\sigma_1 + \sigma_3). \qquad (8)$$

According to the Mohr-Coulomb criterion:

$$\varepsilon_1 - \varepsilon_3 = (\sigma_1 + \sigma_3) \cdot \sin\phi + 2 \cdot c \cdot \cos\phi \qquad (9)$$

a maximum distortion of the elastoplastic border is expressed as:

$$D_{cr} = \frac{1+\nu}{1-\nu} \cdot \sin\phi + 2 \cdot c \cdot \frac{1+\nu}{E} \cdot \cos\phi \qquad (10)$$

with the below material equivalent constants (Table 5).

Table 5. Geomechanical parameters.

Parameters	Units	Values
EP_{LP}	Centimetre	2.5
ν_{LP}	–	0.22
E_{LP}	MPa	15000
σ_{cbp}	MPa	1.04
σ_{tbp}	MPa	0.66

From Eq. (7) and Fig. 22 we obtain:

$$D_{cr} = \theta_v \cdot 1.3021 + 0.0447\,. \qquad (11)$$

The values of the volumetric elongations are taken directly from fixed reference marks on the anchorages in Fig. 20 and are expressed by Eq. (11). If the results obtained are superior to γ_{max} and read on the same signs in Fig. 21, the latter belongs to a plastic zone located on the elasto-plastic deformation border shown in Fig. 23 (see next page). In the opposite case, it is to be found under the same zone and it belongs to an elastic zone. Maximum distortion signs belonging to a plastic zone are connected to mark the border of the plastic zone.

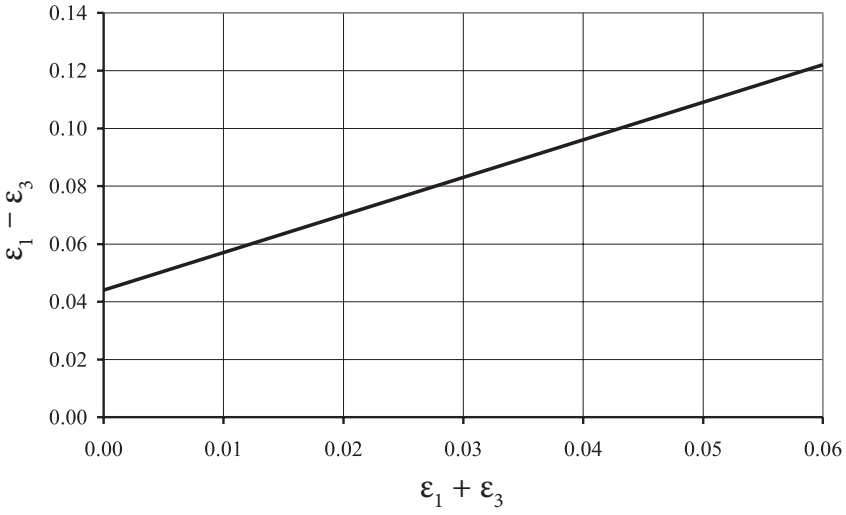

Figure 22. Criterion of the equivalent material rupture.

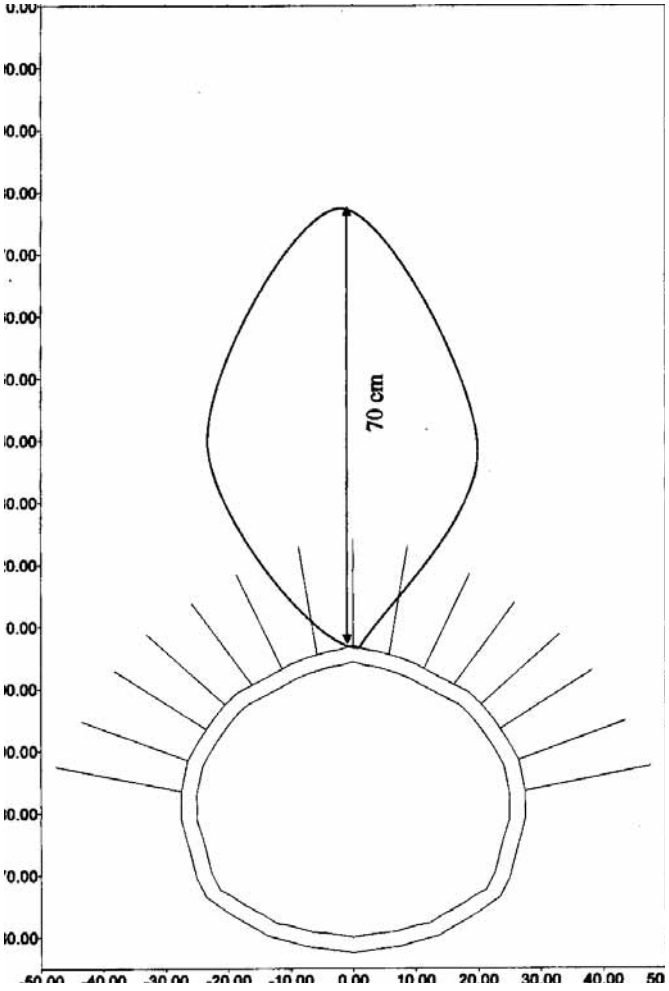

Figure 23. Extension of the plastic zone.

CONCLUSION

The physical model can be directly gauged according to the results of measurements and in situ inspections. The capacity of simulation is based on the capacity of the model equipment to create three- and a two-dimensional field elongations. The investigation confirmed that physical simulations of the rock excavation and supporting systems are effective tools to conceive a proper excavation plan and supporting method of line tunnels.

This research method is able to provide general visual information on the state of the transition process from the excavation of rocks to the supporting systems. It gives a quantitative image of the deformation field and ruptures in each stage of tunnel construction. In this way, a broad deformation was observed at the time of this study which would surely damage the tunnel surface. This broad deformation appeared during the digging stross because of a simultaneous rupture of the injected concrete.

REFERENCES

Adachi, T . and Shinkawa, MR.(1982). Experimental and Analytical study on tunnel support system. *Proc. of the ' HT conf. on num. methods in geomech*, Edmonton, Canada.

Adachi, T. (1985). Some supporting methods for tunnelling in Japan and to their studies. *Rock mechanics suppl., Verlag*.

Baron, K. and Larocque, G. E. (1960). Development of a mine structure. *Wabama report N° 7*, Ottawa, Canada.

Gajari, GY. (1990). Roadway stability investigations by physical and mathematical modelling. *Veszprém Coal Mines*, H-8201 Veszprém, Budapesti u.2, Hungary.

Gerhard S'Mauro F. (1979). Technics and materials for modelling a tunnel drawing operation at moderate depth. *International colloquium on physical geomechanical models*, Bergamo, Italy.

Kozuna, A.M. (1957). Technika modelitovanja ekvalentnuni materialiani. Ugletehizdat Moskva, Russia.

Sakurai,S. (1985). Evaluation of plastic zone around underground opening by means of displacement measurements. *Num. Meth. in geomech. Nagoya*, AA. Balkama Rotterdam, Boston.

Seriani, A. (1993). Seek on equivalent materials for the simulation of tunnel of the subway of Algiers. *Acta Geod. Mount. Hung. Vol. 8*, Academy sciences Hungarian.

Tazawa Y. (1979). Model tests on the effect of rock bolt and thin linings on tunnel supports in soft rock. *Annual report of Kajma institute of construction technology*, Japan.